

Universality of finite-time ray focusing statistics in two-dimensional and one-dimensional potential flows

Sicong Chen  and Lev Kaplan**Department of Physics and Engineering Physics, Tulane University, New Orleans, Louisiana 70118, USA*

(Received 23 January 2024; accepted 26 June 2024; published 23 July 2024)

In the investigation of extreme density or wave height statistics in a disordered medium, of special interest is the search for universal or fundamental properties shared by different types of disorder. In previous work [Chen and Kaplan, *Entropy* **25**, 161 (2023)] we have established a direct connection between the degree of stretching or focusing of ray trajectories and the density distribution. Here we demonstrate the universality of this connection for different physical contexts, and both analytically and numerically show a universal scaling relationship for the stretching exponent distribution in weak, small-angle scattering at finite times for different dispersion relations. We observe that the mean, skewness, and kurtosis of the stretching exponent all display universal nonmonotonic behavior on timescales comparable to the time of first caustic formation, corresponding to the first generation of hot spots in the density profile. In particular, the mean stretching exponent attains negative values before beginning its linear rise at large times. Using the correspondence between two-dimensional small-angle scattering and a one-dimensional kicked model, we show how higher moments of the distribution of the second derivative of the potential affect the statistics of the stretching exponents.

DOI: [10.1103/PhysRevE.110.014211](https://doi.org/10.1103/PhysRevE.110.014211)

I. INTRODUCTION

Ocean waves of extreme height relative to the typical waves in a given sea state are known as freak or rogue waves. Many publicized and documented encounters with extreme oceanic waves have attracted interest over the years, especially in the direction of quantitative predictions for freak wave probability distributions. Commonly used approaches to model freak waves include the Longuet-Higgins random sea model [1], the nonlinear Schrödinger equation (NLS) and its extension in the Dysthe equation [2,3], and ray dynamics as exemplified in the work of White and Fornberg [4].

The Longuet-Higgins random sea model is based on random linear superposition of many plane waves with different direction and wavelength, where the sea surface height at any spatial location behaves, by the central limit theorem, as a Gaussian random variable. In the limit of a narrow frequency spectrum, the crest height then follows a Rayleigh distribution, while observational data [5] show that this purely stochastic Rayleigh model significantly underestimates the actual probabilities of freak waves.

The NLS or the Dysthe equation incorporate nonlinear effects perturbatively and work well in the regime of small or moderate values of wave steepness kH , where H represents wave height and k is the wave number. As nonlinear effects scale as a power of the wave steepness, strong nonlinear evolution is more likely to come from initial conditions with already unusually high waves. In other words, the tail of the crest height distribution is likely to be influenced by linear

triggering mechanisms, even if subsequent nonlinear development is also significant. In the work of White and Fornberg [4], the linear triggering mechanism arises from the focusing or refraction of an incoming plane wave by random current eddies. Whenever a focusing current is present, an incoming sea state develops caustics or singularities with infinite ray density, and consequently a repeated and reproducible pattern of freak waves. Statistics regarding the distribution of crest heights can be obtained by combining the stochastic random seas picture (given by a locally Rayleigh distribution) and the statistics of ray focusing in the presence of random currents [6,7].

Besides extreme waves in the ocean, extreme waves are known to occur in many other physical systems, governed by different equations of motion, where the waves or rays are scattered by a weak random potential. Examples have been reported on a wide range of length scales, including the branching of electron flow [8–12], amplification of tsunami waves [13–15], branching of light traveling through a soap film [16], and freak waves in optical [17,18], acoustic [19,20], and microwave propagation [7,21]. These systems share similarities in statistics and scaling relations, suggesting that a universal theory of scattering in weak random potentials may describe these different phenomena. Indeed, a search for universality in branched flows through potentials with differing correlation structures has obtained success [22,23], including an extension to the anisotropic case [24].

Recently, it was demonstrated that a one-parameter model suffices to describe classical branched flow in a time-dependent 1D random potential, and a two-parameter phase diagram describes the corresponding quantum branched flow [25]. For a recent overview of the theory and applications of branched flow, see Ref. [26].

*Contact author: lkaplan@tulane.edu

In our previous work [27], we have seen that scattering of nonrelativistic particles in a random weak potential field generates density patterns very similar to those observed for deep-water ocean waves in the work of White and Fornberg [4]. Moreover the stretching exponent, a quantity that describes the degree of stretching or focusing of nearby ray trajectories, is explicitly connected to ray densities. This direct connection allows us to treat the stretching exponent [28,29] as a quantitative mirror for the intensity or ray density, so that the statistical distribution of the stretching exponent can reflect the statistics of the density, and therefore also the statistics of wave heights.

In this paper we further explore the statistics of stretching exponents along the forward direction in ray dynamics. Both in different physical contexts associated with diverse dispersion relations and in potentials of differing correlation structures, we are able to demonstrate semianalytically and numerically universal scaling relationships of the stretching exponent for small-angle scattering in weak random potentials. We also observe that particle dynamics in a 2D ray model is, in the regime of small angular spread, analogous to a 1D model with a time-dependent potential. The stretching exponent is mathematically linked to the monodromy matrix, which evolves the phase space displacement vector through time, and therefore the 2D ray dynamics in a random potential is equivalently a problem of random matrix multiplication as observed in Ref. [30]. Whereas the full 4×4 monodromy matrix in 2D space is challenging for numerical evolution and even more so when it comes to an analytical treatment, the 1D model is simple enough to obtain quantitative predictions for the distribution of the stretching exponent. Therefore, we are able to further explore the mechanism and statistics of freak wave events by studying monodromy matrix statistics in the 1D model.

The remainder of this paper is organized as follows: The basic mathematical formalism of monodromy matrices and stretching exponents is reviewed in Sec. II A. Then in Sec. II B we obtain an explicit correspondence for the finite-time evolution of stretching exponent statistics in physical systems described by different dispersion relations, including non-relativistic classical particle flow, deep-water gravity waves, capillary waves, and vibration of membranes. It shown that for small-angle scattering, the statistical distribution of stretching exponents is equivalent for these diverse systems, under an appropriate time or distance rescaling. Then analytical results for the short-time evolution of the mean stretching exponent and its spread are obtained for 1D kicked flow and for flow in a 2D potential.

Numerical results supporting and extending this analysis are presented in Sec. III. The finite-time evolution of the first four moments of the stretching exponent distribution (mean, variance, skewness, and kurtosis) is obtained numerically in Sec. III A and the scaling for different dispersion relations is demonstrated. Notably, the mean, skewness, and kurtosis all display nonmonotonic behavior on timescales comparable to the time of first caustic formation, with the mean stretching exponent attaining negative values before beginning its linear rise at large times. Section III B compares the behavior of 2D potential flow with 1D kicked flow, while the effect of different spatial correlation functions of the random potential

is analyzed in Sec. III C. The effects of non-Gaussian distribution of the second derivative of the random potential V_{xx} are examined in Sec. III D, where we find that the mean value and skewness of the stretching exponent are more sensitive to an asymmetry in the V_{xx} distribution, as compared to the even moments. Finally, Sec. IV summarizes some key results.

II. MODEL AND THEORY

A. Monodromy matrix and stretching exponents

A linear dynamical system in N -dimensional space is governed by $2N$ ordinary differential equations that evolve the $2N$ -dimensional phase space point $\phi = (x^{[1]}, k^{[1]}, \dots, x^{[N]}, k^{[N]})$ in time. This evolution in phase space can be considered as a flow f where $\frac{d\phi}{dt} = f(\phi)$, and in discrete time as a map F from one time point to the next, $\phi_{n+1} = F(\phi_n)$. The flow of the tangent space is a matrix operation acting on a perturbation δ_t of the phase space vector $\phi(t)$,

$$\frac{d\delta_t}{dt} = J(t)\delta_t, \quad (1)$$

where the Jacobian matrix $J(t)$ is

$$J_{ij}(t) = \left. \frac{\partial f_i}{\partial \phi_j} \right|_{\phi=\phi(t)}. \quad (2)$$

Finally, the monodromy or stability matrix $M(t)$, which projects the initial phase space perturbation at time 0 to the phase space perturbation at time t , $\delta_t = M(t)\delta_0$, evolves in accordance with

$$\frac{dM(t)}{dt} = J(t)M(t). \quad (3)$$

Physically, the evolution in phase space occurs in continuous time, but numerical simulations can only take the route of mapping in discrete time. In discrete time, the map F determines the Jacobian matrix K ,

$$K_{ij}(\phi_n) = \left. \frac{\partial F_i}{\partial \phi^{(j)}} \right|_{\phi=\phi_n}, \quad (4)$$

which iterates the tangent space from time step n to $n+1$ as

$$\delta_{n+1} = K(\phi_n)\delta_n. \quad (5)$$

Therefore an initial perturbation δ_0 in the phase space vector is evolved to δ_n at time step n by the monodromy matrix,

$$\delta_n = M_n\delta_0, \quad (6)$$

where

$$M_n = K(\phi_{n-1})K(\phi_{n-2}) \cdots K(\phi_0). \quad (7)$$

The matrix operation M_n or $M(t)$ can be viewed as a linear, canonical transformation with unit determinant, and the eigenvalues come in pairs, $m^{[2j]}(t)m^{[2j+1]}(t) = 1$ (e.g., see Ref. [31], Ch. 5), reducing the effective dimension of the spectrum from $2N$ to N . Moreover, as total energy is a constant of the motion in conservative systems, two of the eigenvalues of $M(t)$ are unity. Therefore in a 2D Hamiltonian system, the eigenvalues of $M(t)$ become $\{m(t), 1/m(t), 1, 1\}$, so that a single parameter $|m(t)|$ solely captures the stability of a trajectory.

In the large-time limit of a weakly disordered system, $|m(t)| \approx \exp(\lambda t)$, where λ is the maximal Lyapunov exponent (MLE), independent of time and independent of the initial conditions. However, we are interested here not in this trivial large-time regime but rather in the finite-time behavior, on timescales comparable to the formation time of the first caustics. As established previously in Ref. [27], the stretching exponents of 2D small-angle scattering in weak random potentials are closely related to the density distribution, as the first generation of caustics is where strongest focusing occurs. Given two ray trajectories $(x_1(t), y_1(t))$, $(x_2(t), y_2(t))$ propagating initially along the y direction and initially slightly separated by δ along the transverse direction x , the degree of stretching or focusing can be quantified by the logarithm of the stretching ratio of the transverse separation:

$$\alpha(t) = \log \left(\left| \frac{x_1(t) - x_2(t)}{x_1(0) - x_2(0)} \right| \right) = \log \left(\frac{|x_1(t) - x_2(t)|}{\delta} \right). \quad (8)$$

The value of the stretching exponent $\alpha(t)$ describes the cumulative exponential divergence or convergence along the transverse direction from time 0 to time t , and its time derivative $d\alpha(t)/dt$ quantifies the rate of exponential divergence or convergence at time t . In the large-time limit, $d\alpha(t)/dt$ approaches the maximum Lyapunov exponent λ of the system. The behavior of the stretching exponent $\alpha(t)$ before reaching the large-time limit is mathematically nontrivial, but previous numerical calculations [27] showed the distribution of the stretching exponent at short and intermediate times. If we adopt phase space coordinates $\phi = (x, k_x, y, k_y)$, the stretching exponent α is also the logarithm of the first element in the monodromy matrix,

$$\alpha(t) = \log(M_{11}(t)). \quad (9)$$

B. Dispersion relations

In the limit of weak (small-angle) scattering, a very wide variety of dispersion relations in two dimensions can be expressed as

$$H = \frac{1}{2} |\vec{k}|^\beta + V(\vec{r}), \quad (10)$$

where the energy or frequency H is conserved and the prefactor $\frac{1}{2}$ is included for mathematical convenience. The vector $\vec{k} = (k_x, k_y)$ is the wave vector or momentum, and the exponent β takes different values depending on the specific physical context. When $\beta = 2$, the dispersion relation describes nonrelativistic classical particles,

$$H = \frac{1}{2} |\vec{k}|^2 + V(\vec{r}), \quad (11)$$

e.g., electrons traveling through a weak potential field. The dispersion relation with $\beta = 1/2$ models deep-water gravity waves where H is the wave frequency [4] [and for a narrow angular trajectory spread, the field $V(\vec{r})$ is proportional to the current in the forward direction]. Other values of β are also commonly found physically, such as in vibrating membranes ($\beta = 1$) and capillary waves ($\beta = 3/2$) [32].

In the following analysis, $V(\vec{r})$ is taken to be a 2D random time-independent disordered potential with zero average,

fluctuations of size σ ($\sigma^2 = \overline{V^2}$), and a spatial correlation function $C(\vec{r})$ characterized by correlation length ξ . Note that when the potential strength σ is small compared to the total energy ($\sigma \ll H$), Eq. (10) may be regarded as the first-order expansion of a more complicated dispersion relation. In the special case of $\beta = 2$ (Eq. (11)), the first caustics appear after a travel distance

$$L \sim \xi(\sigma/H)^{-2/3} \quad (12)$$

along the y direction, where the earliest cusp singularities form [4,12]. More generally, the motion obeys the usual eikonal equations:

$$\frac{d\vec{r}}{dt} = \frac{\partial H}{\partial \vec{k}}, \quad \frac{d\vec{k}}{dt} = -\frac{\partial H}{\partial \vec{r}}. \quad (13)$$

In 2D space and in the limit of weak disorder ($\sigma \ll H$), Eq. (13) can be explicitly written out as

$$\begin{aligned} \frac{dx}{dt} &= \frac{\beta}{2} k_x [2(H - V)]^{1-\frac{2}{\beta}} \approx \frac{\beta}{2} k_x (2H)^{1-\frac{2}{\beta}}, \\ \frac{dy}{dt} &= \frac{\beta}{2} k_y [2(H - V)]^{1-\frac{2}{\beta}} \approx \frac{\beta}{2} k_y (2H)^{1-\frac{2}{\beta}}, \\ \frac{dk_x}{dt} &= -\frac{\partial V}{\partial x}, \quad \frac{dk_y}{dt} = -\frac{\partial V}{\partial y}. \end{aligned} \quad (14)$$

Defining $B = \frac{\beta}{2} (2H)^{1-\frac{2}{\beta}}$, the equations of motions can be reexpressed as

$$\begin{aligned} \frac{dx}{dt} &= Bk_x, \quad \frac{dy}{dt} = Bk_y, \\ \frac{dk_x}{dt} &= -\frac{\partial V}{\partial x}, \quad \frac{dk_y}{dt} = -\frac{\partial V}{\partial y}, \end{aligned} \quad (15)$$

which are the Hamiltonian equations of motion for an effective Hamiltonian

$$\tilde{H} = \frac{B}{2} |\vec{k}|^2 + V(\vec{r}). \quad (16)$$

Thus, motion governed by a dispersion relation of the form of Eq. (10), for any β , is identical to leading order in the potential strength with the motion of nonrelativistic particles with an effective mass $1/B$ in the same disorder. Therefore in the limit of weak scattering, the 2D classical particle model is sufficient for the study of stretching exponent statistics.

Equivalently, it is convenient to note from Eq. (15) or Eq. (16) that the constant B may be eliminated via the transformation $V \rightarrow BV$ and $t \rightarrow t/B$. Thus, the monodromy matrix arising from the dispersion relation (10) in disorder $V(\vec{r})$ at time $N\delta t$ is identical with the monodromy matrix from classical particle mechanics, Eq. (11), in disorder $\tilde{V}(\vec{r}) = V(\vec{r})/B$ at time $N\delta T = BN\delta t$.

Given the distance scaling law shown in Eq. (12), if Hamiltonian motion in disorder $\tilde{V}(\vec{r}) = V(\vec{r})/B$ after time $N\delta T = BN\delta t$ covers a distance associated with the formation of first caustics, so will another Hamiltonian motion with same total energy in disorder $V(\vec{r})$ after time $B^{-2/3}N\delta T = B^{1/3}N\delta t$. In other words these two Hamiltonian motions in disorders $\tilde{V}(\vec{r}) = V(\vec{r})/B$ and $V(\vec{r})$ achieve the same monodromy matrix at times $BN\delta t$ and $B^{1/3}N\delta t$, respectively. Now, using the equivalence between Hamiltonians (11) and (16), we find that

motion governed by the general dispersion relation (10) in disorder $V(\vec{r})$ achieves the same monodromy matrix after time $N\delta t$ as does nonrelativistic particle dynamics (11) in the same disorder $V(\vec{r})$ after time $B^{1/3}N\delta t$. Note that the equivalence relies on the assumptions of weak disorder and narrow angular ray spread.

Since rays under the classical particle dispersion relation (10) are propagating forward with momentum $(2H)^{1/2}$, the distance scale associated with caustic formation is given for general β by

$$L_\beta \sim B^{1/3}\xi(\sigma/H)^{-2/3} \\ \sim \xi(\sigma/H)^{-2/3}(\beta H)^{1/3}(2H)^{-\frac{2}{3\beta}}, \quad (17)$$

which of course is equivalent to the simpler form (12) for the special case $\beta = 2$. This rescaling—the key result of this subsection—bridges different dispersion relations and greatly simplifies the analysis of 2D weak random scattering, because both the distribution of stretching exponents and the density distribution for the general situation described by Eq. (10) may be expressed in terms of the corresponding behavior for the special situation of classical particle motion, Eq. (11).

C. Stretching exponent statistics for 1D kicked model and 2D scattering

Mathematically, because the stretching exponent is given by the logarithm of one element of the monodromy matrix [see Eq. (9)], the statistics of the stretching exponent over time in weak random potentials are to be obtained from the statistics of the evolving monodromy matrix, which for a disordered potential may be viewed as a product of random Jacobian matrices drawn from a certain statistical distribution. More specifically, it is the distribution and correlation of second derivatives of the potential, V_{xx} , V_{xy} , and V_{yy} , that directly determine the statistics of the monodromy matrix.

In 2D dynamics, the analysis requires multiplication of 4×4 matrices with random matrix elements, which is a relatively challenging problem to treat. Hence we first approach the evolution of the stretching exponent in a simple model of one-dimensional Hamiltonian motion in a time-dependent potential $H(t) = \frac{1}{2}k^2 + V(x, t)$, where the single spatial dimension x corresponds to the transverse dimension in 2D small-angle scattering, and the time parameter is analogous to the forward direction y .

1. 1D kicked model

In the 1D model, the Jacobian matrices and the monodromy matrix have dimension 2 instead of 4. The Jacobian matrix that evolves the phase space displacement vector $\begin{pmatrix} \delta x \\ \delta k \end{pmatrix}$ by one step takes the form $K(t) = \begin{bmatrix} 1 & \delta t \\ -V_{xx}(x, t)\delta t & 1 - V_{xx}(x, t)\delta t \end{bmatrix}$. Without loss of generality, we may choose units where $\delta t = 1$, so that the Jacobian matrix further simplifies to

$$K(t) = \begin{bmatrix} 1 & 1 \\ -V_{xx}(x, t) & 1 - V_{xx}(x, t) \end{bmatrix}. \quad (18)$$

This model can be viewed as a kicked model where $V_{xx}(x, t)$ is the derivative of a single kick. The monodromy matrix after N steps is given by $M_N = \prod_{i=0}^{N-1} K_i$ and the stretching ratio

$e^\alpha = (M_N)_{11}$ is expressed as follows:

$$e^\alpha = 1 - \sum_{i=1}^N (N-i)v_i + \sum_{1 \leq i < j \leq N} (j-i)(N-j)v_i v_j \\ - \sum_{1 \leq i < j < k \leq N} (k-j)(j-i)(N-k)v_i v_j v_k + \dots, \quad (19)$$

where we employ the notation $v_i = V_{xx}|_{x_i, t_i}$.

For times $N \ll T_L$, where T_L is the Lyapunov timescale, we are in the short-time regime $|\alpha| \ll 1$. Here the stretching exponent α may be expanded as a power series in v ,

$$\alpha \approx - \sum_{i=1}^N (N-i)v_i + \sum_{1 \leq i < j \leq N} (j-i)(N-j)v_i v_j \\ - \frac{1}{2} \left[- \sum_{i=1}^N (N-i)v_i + \sum_{1 \leq i < j \leq N} (j-i)(N-j)v_i v_j \right]^2. \quad (20)$$

Naturally there are two aspects of $v_i(x, t)$ that affect the statistics of the stretching exponent α : the distribution of individual kick strengths $v_i(x, t)$ and the time correlation among them. Note that the distance traveled in the 1D kicked model is negligible at short times, so the spatial correlations are not relevant and only the time correlation of the potential contributes to the development of the stretching exponent. Let us first assume no time correlation in the potential and also assume that the distribution of kicks v is symmetric around 0 with variance σ_v^2 . Then the average and variance of the stretching exponent are obtained to first order in σ_v^2 as

$$\bar{\alpha} \approx -\frac{1}{12}(2N^3 + 3N^2 + N)\sigma_v^2 \approx -\frac{1}{6}N^3\sigma_v^2 \\ \overline{(\alpha - \bar{\alpha})^2} \approx \frac{1}{6}(2N^3 + 3N^2 + N)\sigma_v^2 \approx \frac{1}{3}N^3\sigma_v^2. \quad (21)$$

We notice that these expressions are consistent with the Lyapunov time scaling as $T_L \sim \sigma_v^{-2/3}$, in agreement with Eq. (12). For short times $N \ll T_L$, we have stretching exponent $\alpha \ll 1$, and at times of order the Lyapunov time, $N \sim T_L$, the mean and variance of α are of order unity, as expected.

We now introduce a time correlation in the potential with time scale ξ_T in units of the time step ($\xi_T \gg 1$). Here we are interested only in the scaling behavior, so we are not concerned with the precise form of the correlation function. To leading order, the effect of a time-correlated potential is that averages of the form $\sum_{i,j=1}^N \overline{v_i v_j} \sim N\sigma_v^2$ in the uncorrelated case become $\sum_{i,j=1}^N \overline{v_i v_j} \sim N\xi_T\sigma_v^2$ when terms $|i-j| \sim \xi_T$ contribute to the sum. Thus, for a time-correlated potential, the kick strength is effectively rescaled as $\sigma_v^2 \rightarrow \xi_T\sigma_v^2$ and the leading behavior in Eq. (21) for the average and variance of the stretching exponent generalizes to

$$\bar{\alpha} \sim N^3\xi_T\sigma_v^2, \\ \overline{(\alpha - \bar{\alpha})^2} \sim N^3\xi_T\sigma_v^2. \quad (22)$$

Again, the Lyapunov time scale corresponds to the value of N at which the mean exponent $\bar{\alpha}$ reaches values of order unity, i.e., $T_L \sim \xi_T^{-1/3}\sigma_v^{-2/3}$.

2. 2D scattering

We now return to the 2D Hamiltonian motion described by the Hamiltonian of Eq. (11). Using coordinates $\phi = (x, y, k_x, k_y)$, the Jacobian matrix for a single time step $\delta t = 1$ can be written, in analogy with Eq. (18) for the 1D case, as

$$K = \begin{bmatrix} 1 & 0 & 1 & 0 \\ 0 & 1 & 0 & 1 \\ -V_{xx} & -V_{xy} & 1 - V_{xx} & -V_{xy} \\ -V_{xy} & -V_{yy} & -V_{xy} & 1 - V_{yy} \end{bmatrix} = \begin{bmatrix} I_2 & I_2 \\ \epsilon & I_2 + \epsilon \end{bmatrix}, \quad (23)$$

where I_2 is the 2×2 identity matrix and $\epsilon = \begin{bmatrix} -V_{xx} & -V_{xy} \\ -V_{xy} & -V_{yy} \end{bmatrix}$.

The randomness of the Jacobian matrices arises from the randomness of the second derivatives V_{xx} , V_{yy} , and V_{xy} . Then, for times short compared with the Lyapunov time, the upper-left 2×2 block of the monodromy matrix, which acts on the position coordinates (x, y) , may be written as

$$M_{\text{sub}} = 1 + \sum_{i=1}^N (N-i)\epsilon_i - \sum_{1 \leq i < j \leq N} (j-i)(N-j)\epsilon_i \epsilon_j + \sum_{1 \leq i < j < k \leq N} (k-j)(j-i)(N-k)\epsilon_i \epsilon_j \epsilon_k + \dots, \quad (24)$$

in full analogy with Eq. (19). Specifically, the first element $M_{11} = e^\alpha$ of the monodromy matrix takes the form

$$M_{11} = 1 - \sum_{i=1}^N (N-i)V_{xx,i} + \sum_{1 \leq i < j \leq N} (j-i)(N-j)(V_{xx,i}V_{xx,j} + V_{xy,i}V_{xy,j}) - \dots, \quad (25)$$

where $V_{xx,i}$ is the second derivative with respect to x at position (x_i, y_i) , which is the trajectory position at time step i , and similarly for $V_{xy,i}$. Therefore, the stretching exponent α may be expanded at short times as

$$\alpha \approx - \sum_{i=1}^N (N-i)V_{xx,i} + \sum_{1 \leq i < j \leq N} (j-i)(N-j) \times (V_{xx,i}V_{xx,j} + V_{xy,i}V_{xy,j}) - \frac{1}{2} \left[- \sum_{i=1}^N (N-i)V_{xx,i} + \sum_{1 \leq i < j \leq N} (j-i)(N-j) \times (V_{xx,i}V_{xx,j} + V_{xy,i}V_{xy,j}) \right]^2. \quad (26)$$

We now take the random 2D potential $V(x, y)$ to be a superposition of many independent random potential bumps at randomly chosen locations (x_i, y_i) :

$$V(x, y) = \sum_{i=1}^n h_i U(x - x_i, y - y_i). \quad (27)$$

The number of bumps is taken to be sufficiently large so that the bumps are strongly overlapping—in other words, the typical interbump separation is small compared to the extent

of the bump shape U . The bump shape U , which for simplicity is taken to be symmetric in both x and y , determines the correlation function of the potential, i.e., the potential is white noise convolved with U . By the central limit theorem the derivatives of the potential at any location will be distributed as Gaussian variables with zero mean. Under these conditions, the mean stretching exponent may be written as

$$\begin{aligned} \bar{\alpha} &\approx \sum_{1 \leq i \leq j \leq N} -(N-j)^2 \overline{V_{xx,i}V_{xx,j}} \\ &+ \sum_{1 \leq i < j \leq N} (j-i)(N-j) \overline{V_{xy,i}V_{xy,j}} \\ &\approx - \int_0^N dj \int_0^j di (N-j)^2 \overline{V_{xx,i}V_{xx,j}} \\ &+ \int_0^N dj \int_0^j di (j-i)(N-j) \overline{V_{xy,i}V_{xy,j}}, \end{aligned} \quad (28)$$

where in the last step we have introduced a continuum time limit, valid when the time step is small compared to the time associated with traversing a single bump.

Before proceeding with the calculation, we introduce the two-point correlation function of the potential $V(x, y)$,

$$C(\Delta x, \Delta y) = \frac{\overline{V(x_0 + \Delta x, y_0 + \Delta y)V(x_0, y_0)}}{\overline{V^2(x_0, y_0)}}, \quad (29)$$

which depends only on the bump shape U . Specifically, starting with the construction of the potential $V(x, y)$ given in Eq. (27) and replacing the sums over $x' = x - x_i$, $y' = y - y_i$ by integrals, we have

$$\begin{aligned} C(\Delta x, \Delta y) &\sim \iint dx' dy' U(x', y') U(x' + \Delta x, y' - \Delta y) \\ &= \iint dx' dy' U(-x', -y') U(x' + \Delta x, y' - \Delta y), \end{aligned} \quad (30)$$

where we have dropped a normalization constant, fixed of course by $C(0, 0) = 1$, and where in the second line we have used the reflection symmetry of U . Thus, C is simply the convolution of the bump size U with itself. Furthermore, the convolution theorem implies $\mathcal{F}[C] \sim (\mathcal{F}[U])^2$, where \mathcal{F} is the Fourier transform, allowing the construction of the potential bump shape from the correlation function as

$$U(\Delta x, \Delta y) \sim \mathcal{F}^{-1}[\sqrt{\mathcal{F}[C(\Delta x, \Delta y)]}]. \quad (31)$$

However, the stretching exponent is not directly related to the values of the potential $V(x, y)$ and instead is determined by strength of the *second derivatives* of the potential and the correlations among them. Since the derivatives of the full potential are given by sums over bumps, $V_{xx}(x, y) = \sum_{i=1}^n h_i U_{xx}(x - x_i, y - y_i)$, and the bumps are uncorrelated, all calculations (up to normalization) can be based on a single potential bump. In Fourier space, the second derivative $v(x, y) = V_{xx}(x, y)$ becomes $\mathcal{F}[v](z, w) = (iz)^2 \mathcal{F}[V](z, w)$, and using Eq. (31),

$$\mathcal{F}[v](z, w) \sim (iz)^2 \sqrt{\mathcal{F}[C](z, w)}. \quad (32)$$

The other second derivatives may be obtained similarly. Continuing to take $v = V_{xx}$ as an example, the correlation function

$c(\Delta x, \Delta y)$ may be defined as

$$c(\Delta x, \Delta y) = \frac{V_{xx}(x_0 + \Delta x, y_0 + \Delta y)V_{xx}(x_0, y_0)}{V_{xx}^2(x_0, y_0)}. \quad (33)$$

Setting aside the normalization constant, in Fourier space we have

$$\mathcal{F}[c] \sim (\mathcal{F}[v])^2 \sim (iz)^4 \mathcal{F}[C] = \mathcal{F}\left[\frac{\partial^4 C(\Delta x, \Delta y)}{\partial \Delta x^4}\right]. \quad (34)$$

Therefore the correlation function of the second derivatives v is connected to the correlation function of the potential V itself via

$$c(\Delta x, \Delta y) = \frac{\frac{\partial^4 C(\Delta x, \Delta y)}{\partial \Delta x^4}}{\frac{\partial^4 C(\Delta x, \Delta y)}{\partial \Delta x^4} \Big|_{\Delta x = \Delta y = 0}}, \quad (35)$$

where we have inserted the correct normalization factor, and the normalized correlation functions of V_{yy} and V_{xy} are given similarly.

Having obtained explicit expressions for the relevant correlation functions, we now return to our goal—the development of the stretching exponent α . In the regime where time is short compared with the Lyapunov time but still large compared to the time needed to traverse a single correlation length of the potential (so that a statistical treatment of trajectories is appropriate), the second term in Eq. (28) will be negligible compared with the first,

$$\bar{\alpha} \approx -\overline{V_{xx}^2} \int_0^N (N-j)^2 \int_0^j c(x_j - x_i, y_j - y_i) di dj. \quad (36)$$

Furthermore, when the angular spread of trajectories is narrow and the potential is weak, the forward distance traveled is approximately proportional to time, $y_j - y_i \approx k_y(j-i) \approx \sqrt{2H}(j-i)$, and the distance traveled in the transverse direction remains small (compared to the potential correlation length), so the result simplifies further to

$$\begin{aligned} \bar{\alpha} &\approx -\overline{V_{xx}^2} \int_0^N (N-j)^2 dj \frac{1}{\sqrt{2H}} \int_0^\infty c(0, \Delta y) d\Delta y \\ &= -\frac{N^3}{3} \frac{\overline{V_{xx}^2}}{\sqrt{2H}} \int_0^\infty c(0, \Delta y) d\Delta y. \end{aligned} \quad (37)$$

The mean square of V_{xx} in 2D scattering is proportional to the strength of the potential,

$$\begin{aligned} \overline{V_{xx}^2} &= \frac{\sigma^2}{\iint V^2(x, y) dx dy} \iint V_{xx}^2(x, y) dx dy \\ &= \sigma^2 \frac{\partial^4 C(\Delta x, \Delta y)}{\partial \Delta x^4} \Big|_{\Delta x = \Delta y = 0}, \end{aligned} \quad (38)$$

where σ^2 is the mean-square strength of the random potential. The effective length scale that appears in Eq. (37) and describes the effect of the correlated potential is given by

$$\int_0^\infty c(0, \Delta y) d\Delta y = \int_0^\infty \frac{\frac{\partial^4 C(\Delta x, \Delta y)}{\partial \Delta x^4} \Big|_{\Delta x=0}}{\frac{\partial^4 C(\Delta x, \Delta y)}{\partial \Delta x^4} \Big|_{\Delta x = \Delta y = 0}} d\Delta y. \quad (39)$$

Therefore in the regime of small-angle scattering and weak potential, the average stretching exponent at short times is

obtained by substituting Eqs. (38) and (39) into Eq. (37),

$$\bar{\alpha} \approx -\frac{\sigma^2 N^3}{3\sqrt{2H}} \int_0^\infty \frac{\partial^4 C(\Delta x, \Delta y)}{\partial \Delta x^4} \Big|_{\Delta x=0} d\Delta y. \quad (40)$$

Although this scaling relationship is only obtained here for short times, we will see in Sec. III that the same distance scaling factor

$$R_C = \int_0^\infty \frac{\partial^4 C(\Delta x, \Delta y)}{\partial \Delta x^4} \Big|_{\Delta x=0} d\Delta y, \quad (41)$$

which has been introduced for example in Refs. [4,33], remains valid at intermediate and large timescales. Indeed, we will observe in Sec. III that not only $\bar{\alpha}$ but the entire distribution of the stretching exponent α behaves universally under the rescaling given by Eq. (41).

Now, from Eq. (40) we see that the length associated with the stretching exponent reaching values of order unity (equivalently, the distance scale to the first caustics) scales as

$$\begin{aligned} L_{\alpha \sim 1} &\approx \sqrt{2H} N_{\alpha \sim 1} \\ &\sim \left(\frac{\sigma}{H}\right)^{-2/3} \left(\int_0^\infty \frac{\partial^4 C(\Delta x, \Delta y)}{\partial \Delta x^4} \Big|_{\Delta x=0} d\Delta y\right)^{-1/3}. \end{aligned} \quad (42)$$

We note that the last factor in Eq. (42) may be interpreted as a correlation length, and thus this expression is in full agreement with the expected scaling given above in Eq. (12). Similarly, the maximum Lyapunov exponent scales as

$$\lambda \sim \left(\frac{\sigma}{H}\right)^{2/3} \left(\int_0^\infty \frac{\partial^4 C(\Delta x, \Delta y)}{\partial \Delta x^4} \Big|_{\Delta x=0} d\Delta y\right)^{1/3}. \quad (43)$$

Such a scaling relationship is consistent with the scaling law for the maximal Lyapunov exponent seen in previous works [30].

We remark that the derivation leading up to Eqs. (40), (42), and (43) relies on the assumption of vanishing average for V_{xx} . When V_{xx} has nonzero average, for example, in the case of harmonic transverse confinement $V(x, y) = \frac{k}{2}x^2 + \dots$, faster divergence from the universal pattern may be expected. Also universal development of the stretching exponent distribution is not expected to hold when V_{xx} is not normally distributed. The question of possible deviations associated with higher moments of the V_{xx} distribution is addressed in Sec. III D.

III. NUMERICAL RESULTS AND DISCUSSION

The analysis in Sec. II suggests that the distribution of stretching exponents in 2D scattering may be universal under the conditions of weak correlated disorder and small angular spread, and in particular that this distribution may be independent of the dispersion relation (Sec. II B) and also of the form of the disorder correlation (Sec. II C), after appropriate rescaling.

A. Varying dispersion relations

Here we begin by computing moments of the stretching exponent for evolution in a random potential $V(\vec{r})$ under dispersion relations given by Eq. (10) for several different values of the β parameter. Without loss of generality, the numerical

value of H is set to unity in each case. The 2D random potentials are constructed to be locally Gaussian with zero mean and variance σ^2 , and to have Gaussian spatial correlation, $C(\vec{r}) = e^{-|\vec{r}|^2/\xi^2}$.

In the simulation, pairs of trajectories are propagated forward along the y direction through the random potential with small initial separation δ in the transverse direction x , and the stretching exponent is calculated as $\alpha(t) = \log(|x_1(t) - x_2(t)|/\delta)$. For each realization of the random potential, we propagate the pairs of ray trajectories under the appropriate dispersion relation, compute the stretching exponents, and associate these exponents α with positions (x, y) . Then the moments of α are computed as functions of the forward distance y by averaging over the transverse position x and over the disorder ensemble. The minimum value of the average stretching exponent occurs around $y = 42$, $y = 80$, $y = 100$, and $y = 130$ (in units of the grid spacing) for dispersion relations described by $\beta = 0.5$, $\beta = 1.5$, $\beta = 2$, and $\beta = 3$, respectively. The forward distance is then rescaled in accordance with Eq. (17), and the results are displayed in Fig. 1. Here Fig. 1(a) shows the mean $\bar{\alpha}$ (lower curves) and the variance $\sigma_\alpha^2 = \overline{(\alpha - \bar{\alpha})^2}$ (upper curves), while Fig. 1(b) shows the normalized skewness $\overline{(\alpha - \bar{\alpha})^3}/\sigma_\alpha^3$ (lower curves) and kurtosis $\overline{(\alpha - \bar{\alpha})^4}/\sigma_\alpha^4$ (upper curves). We find excellent agreement with the predicted scaling for all moments except in the case of the smallest value of the power β , $\beta = 0.5$. Of course, the scaling relationship given in Eq. (17) is expected to work perfectly only in the limit of very weak potential. Keeping subleading terms omitted in Eq. , we would obtain

$$\begin{aligned} \frac{dx}{dt} &\approx \frac{\beta}{2}(2H)^{1-\frac{2}{\beta}} \left[1 - \left(1 - \frac{2}{\beta} \right) \frac{V}{H} \right] k_x, \\ \frac{dy}{dt} &\approx \frac{\beta}{2}(2H)^{1-\frac{2}{\beta}} \left[1 - \left(1 - \frac{2}{\beta} \right) \frac{V}{H} \right] k_y, \end{aligned} \quad (44)$$

where the correction $-(1 - \frac{2}{\beta})\frac{V}{H}$ grows with decreasing β values: $-\frac{1}{3}\frac{V}{H}$, 0 , $\frac{1}{3}\frac{V}{H}$, $3\frac{V}{H}$ for $\beta = 3, 2, \frac{3}{2}, \frac{1}{2}$ respectively. Thus, other things being equal, a smaller potential strength is required to recover universal behavior for small values of β . In Fig. 1 the predicted scaling factor works very well for potentials of strength $\sigma = 0.025$ for $\beta = \frac{3}{2}, 2, 3$, and the case $\beta = \frac{1}{2}$ would require an even weaker potential for full quantitative agreement. In any case, we confirm that in the regime of small angular spread and sufficiently weak potential, the distribution of stretching exponents and the time evolution of this distribution are universal for different equations of motion. Therefore, in the following studies we can use the motion of nonrelativistic classical particles without loss of generality.

B. Comparison with 1D kicked model

We have seen in Sec. II C that the 1D kicked model in a time-dependent weak potential is analogous to small-angle 2D scattering in a weak potential. Further numerical results displayed in Fig. 2 show that even without time correlation of the 1D potential, 1D kicked motion gives rise to the same pattern of stretching exponents as in 2D scattering. Here the evolution of monodromy matrix $M_N = \prod_{i=0}^{N-1} K_i$ is simulated

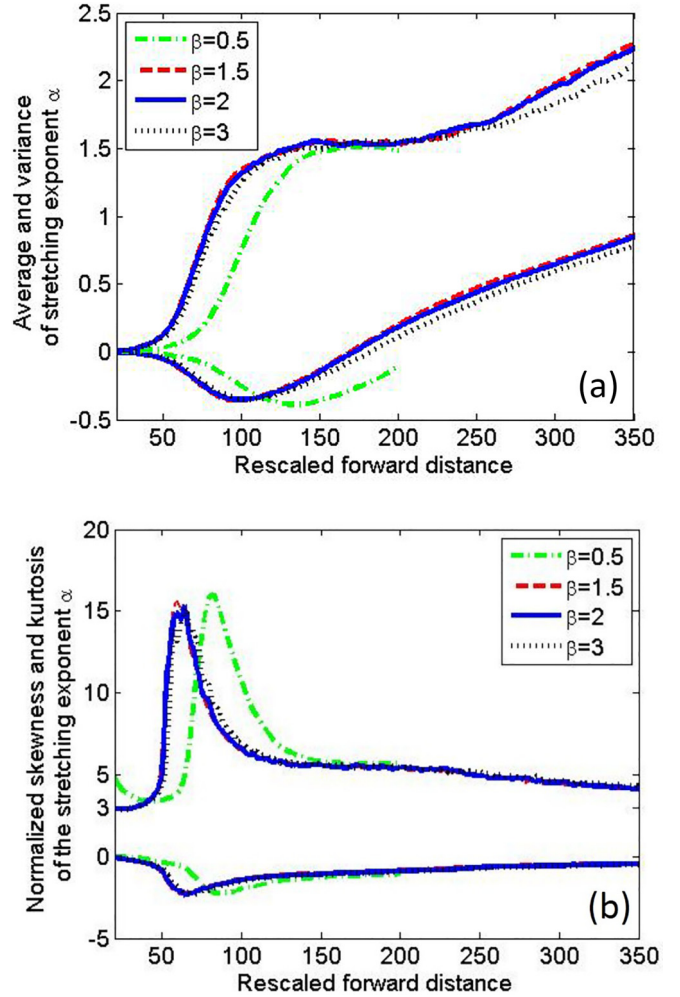


FIG. 1. Moments of the stretching exponent α in 2D scattering for different dispersion relations given by Eq. (10) with $\beta = 0.5, 1.5, 2, 3$. In each case, the value of H is set to unity. The potentials are Gaussian random with mean 0, rms potential strength $\sigma = 0.025$, and Gaussian correlation $C(\vec{r}) = e^{-|\vec{r}|^2/\xi^2}$, where $\xi = 10$ in units of the grid spacing. All data are collected on a 512×512 potential field. Panel (a) shows the mean (lower curves) and variance (upper curves) of the stretching exponent α , and panel (b) shows the normalized skewness (lower curves) and kurtosis (upper curves).

by multiplication of random Jacobian matrices of the form (18), where each individual kick V_{xx} is drawn independently from a normal distribution with standard deviation $\sigma_v \ll 1$. The moments of the stretching exponent $\alpha = \log(M_{11})$ are then computed by averaging over an ensemble of sequences of random individual kicks. Up to a scaling factor of order unity, the independent kick model is physically equivalent to a correlated kick model where the correlation time is of the order of one time step [see Eq. (22)]. Since this random kicked model does not involve propagating the phase space trajectory by integrating the equations of motions in a potential over time, it provides a great numerical advantage in studying the relationship between the stretching exponents and the distribution of V_{xx} .

In fact, if we rescale the 1D data numerically along the forward direction, by matching the location of the minimum in the average stretching exponent curve to the 2D data, we

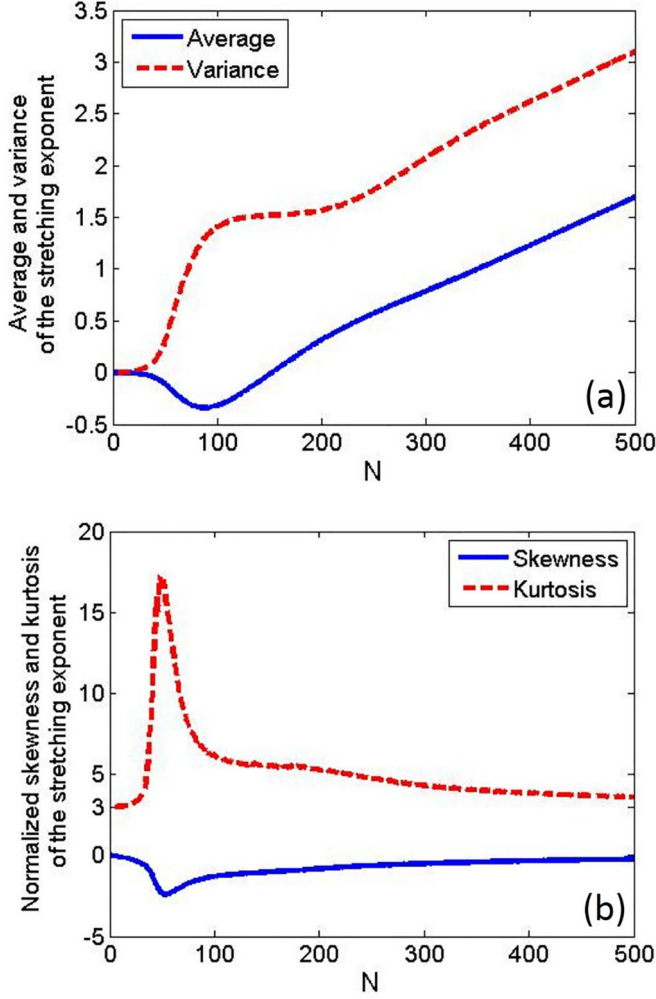


FIG. 2. Moments of the stretching exponent α in the 1D model with uncorrelated kicks ($\sigma_v = 0.002$). Panel (a) shows the development of the mean and variance of the stretching exponent, and panel (b) shows the normalized skewness and kurtosis as defined in the text.

find that the moments of the stretching exponent statistics in small-angle 2D scattering are in excellent agreement with those obtained from the uncorrelated 1D model, as seen in Fig. 3. Of course, this correspondence with 1D motion is valid only in the regime of small angular spread. For larger angular spread, the connection between 2D scattering and the 1D kicked model will be broken.

C. Varying correlations

We now investigate the effect of potential correlations. The 2D random potential $V(x, y)$ can be considered to be a superposition of many potential bumps of identical shape and random, independent heights as in Eq. (27). We focus here on the case where the bump heights follow a symmetric distribution and the bumps are strongly overlapping, so that by the central limit theorem the derivatives of V (as well as V itself) follow a normal distribution. In this scenario, the two major parameters that tune the length scale for the stretching exponent evolution are the variance of the second derivatives V_{xx} and the correlation function of V_{xx} , as shown in Eq. (37).

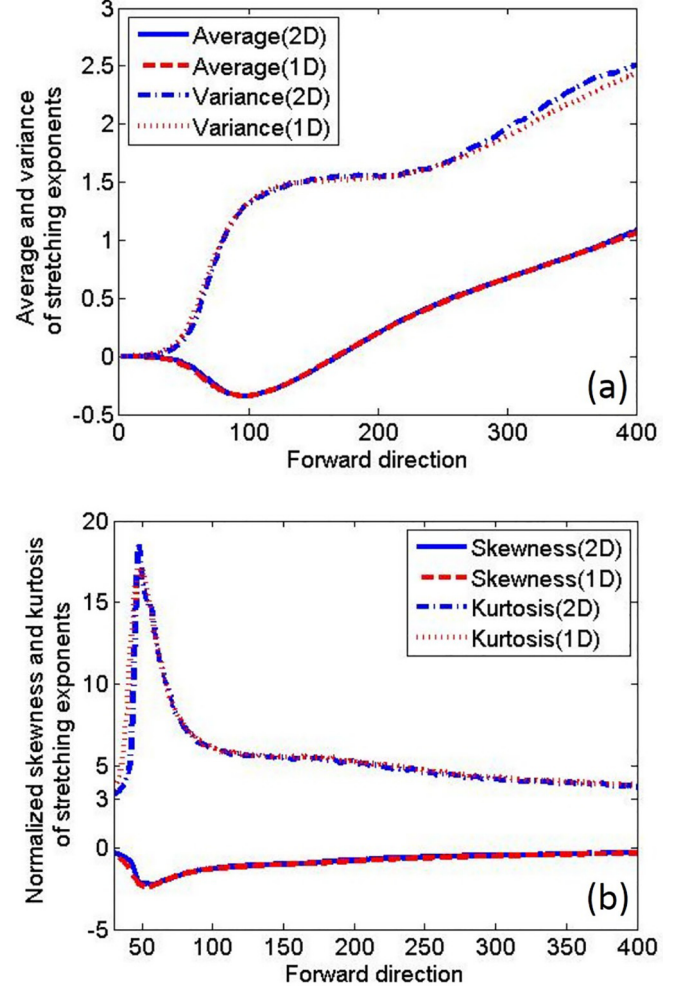


FIG. 3. Numerically rescaled stretching exponent statistics in the 1D uncorrelated kick model ($\sigma_v = 0.002$) and in 2D small-angle scattering in a Gaussian random potential with Gaussian correlations (rms potential strength $\sigma = 0.025$; potential correlation length $\xi = 10$). The 1D data are as in Fig. 2 but rescaled along the horizontal axis so that the minimum in the mean stretching exponent curve is at the same distance from the origin as the minimum in the 2D data.

Numerically, the bump shape is chosen to obey a specific correlation function via Eq. (31), and the bumps are then superposed with random heights to construct a realization of the full potential,

$$V(\vec{r}) = \mathcal{F}^{-1}[\sqrt{\mathcal{F}[C(\vec{r})]} \mathcal{F}[g(\vec{r})]], \quad (45)$$

where $g(\vec{r})$ represents white noise (numerically $g(\vec{r}) = \sum_{i=1}^N h_i \delta(\vec{r}_i)$ with h_i uniformly distributed in $[-1, 1]$). We choose several types of potential correlation functions: a Gaussian function, a sech function, and inverse polynomials (referred to as “power” correlations in the following):

$$\begin{aligned} C(\vec{r}) &= e^{-|\vec{r}|^2/\xi^2}, \\ C(\vec{r}) &= \text{sech}(|\vec{r}|/\xi), \\ C(\vec{r}) &= \frac{1}{1 + (|\vec{r}|/\xi)^a} \quad (a = 1, 2, 3, 4). \end{aligned} \quad (46)$$

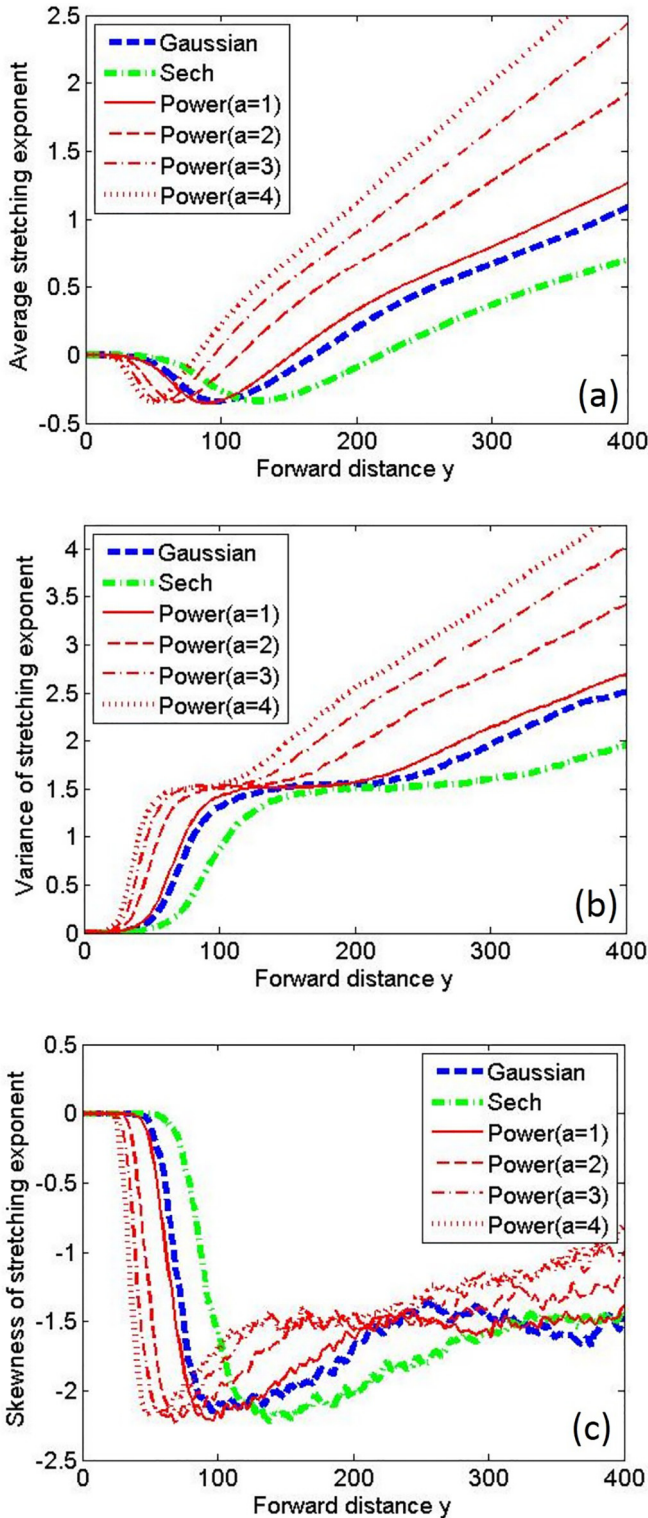


FIG. 4. Moments of the stretching exponent α for 2D scattering in random potentials chosen to obey six different correlation functions ($\sigma = 0.025$, $\xi = 10$). Panels (a), (b), and (c) show, respectively, the average, variance, and normalized skewness of the stretching exponent α .

Moments of the stretching exponents along the transverse direction are shown in Fig. 4. The maximal focusing as determined by a minimum in the mean stretching exponent

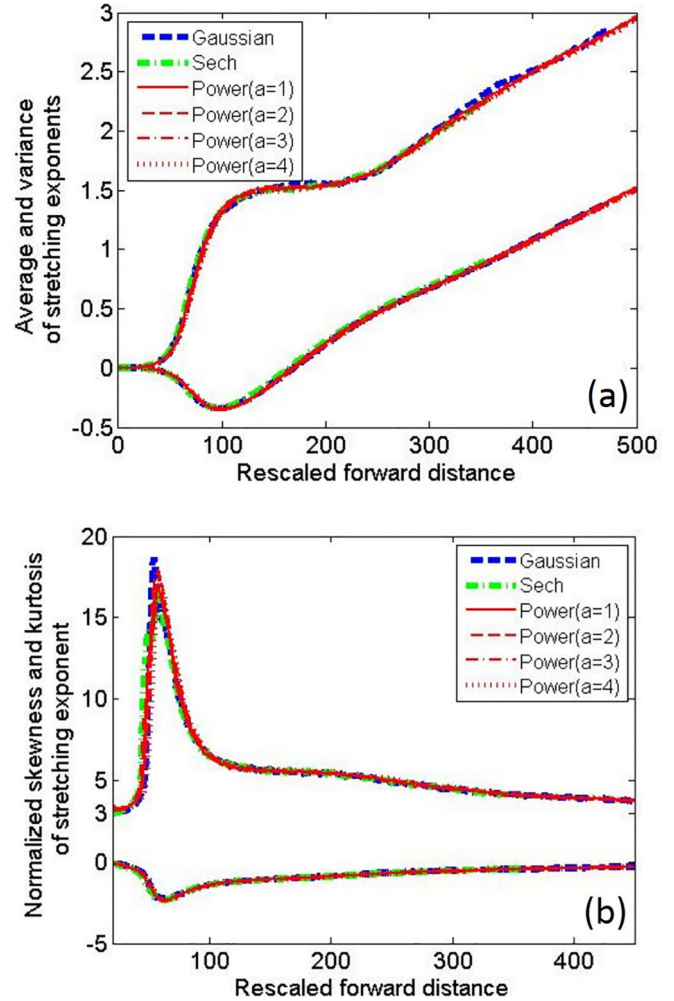


FIG. 5. Moments of the stretching exponents α for 2D scattering in random potentials as in Fig. 4, but with the forward distance rescaled in accordance with Eq. (41). Panel (a) shows the mean (lower curves) and variance (upper curves) of α . Panel (b) shows the normalized skewness (lower curves) and normalized kurtosis (upper curves) of α .

occurs around $y = 97$, $y = 130$, $y = 90$, $y = 67$, $y = 56$, and $y = 49$ (in units of the grid spacing) for Gaussian correlations, sech correlations, and power correlations with $\alpha = 1, 2, 3, 4$ respectively. Since the scaling with the potential strength σ is well established [see Eqs. (12) and (17)], σ is fixed in the calculation. In Fig. 5 the forward distance is rescaled by the factor R_C for each correlation function C as indicated in Eq. (41). Excellent correspondence after rescaling confirms analytical predictions of a universal scaling relationship for different random disorders. Notably, while the formal derivation leading up to Eq. (41) is valid only at times small compared to the Lyapunov time, the results in Fig. 5 indicate that the rescaling remains valid at much larger times. Given this universality, we can then predict the locations of the first caustics or extreme intensities in any random disorder.

We now connect the statistics of the stretching exponent with the maximum Lyapunov exponent (MLE) λ of a given system, which describes the motion in the limit of large times

TABLE I. The maximal Lyapunov exponent λ , before and after rescaling by the scaling factor Z defined in Eq. (47), is shown for the six potential correlation functions displayed in Eq. (46). In each case, the potential is of strength $\sigma = 0.025$, with correlation scale $\xi = 10$. The exponent λ for each type of correlation function is obtained by averaging over 30 realization of a disorder ensemble.

Correlation function	Z	λ	λ/Z
Gaussian	0.02985	0.006792	0.2276
Sech	0.02256	0.005275	0.2338
Power($a = 1$)	0.03281	0.007625	0.2323
Power($a = 2$)	0.04454	0.01046	0.2348
Power($a = 3$)	0.05367	0.01254	0.2337
Power($a = 4$)	0.06144	0.01484	0.2415

(or equivalently here, in the limit of large forward distance). While analytically solving for λ in a given scattering system may not be possible, we can make use of the relation $\alpha \sim \lambda y$ for large forward distance y , and obtain λ by performing a linear fit of $\alpha(y)$ [see Fig. 4(a)] in the large y regime. The numerical values of the MLE obtained from this fitting procedure for the six different correlation functions are displayed in Table I. The calculated scaling factors

$$Z = \left(\frac{\sigma}{H}\right)^{2/3} \left(\int_0^\infty \frac{\partial^4 C(\Delta x, \Delta y)}{\partial \Delta x^4} \Big|_{\Delta x=0} d\Delta y \right)^{1/3} \quad (47)$$

and the rescaled MLE values λ/Z are also shown in Table I. Therefore we obtain an accurate approximation of the maximum Lyapunov exponent,

$$\lambda \approx 0.234 \left(\frac{\sigma}{H}\right)^{2/3} \left(\int_0^\infty \frac{\partial^4 C(\Delta x, \Delta y)}{\partial \Delta x^4} \Big|_{\Delta x=0} d\Delta y \right)^{1/3} \quad (48)$$

(with fluctuations less than 5% of the average value). Equivalently, the forward distance to the first caustics from initially parallel trajectories may be obtained as

$$L \approx 2.96 \left(\frac{\sigma}{H}\right)^{-2/3} \left(\int_0^\infty \frac{\partial^4 C(\Delta x, \Delta y)}{\partial \Delta x^4} \Big|_{\Delta x=0} d\Delta y \right)^{-1/3}, \quad (49)$$

to be compared with Eq. (42).

D. Non-Gaussian potential distributions

The distribution of second derivatives of the potential and their correlation jointly determine the evolution of the stretching exponents. While the average of the second derivative V_{xx} vanishes as long as V_x is bounded, higher moments of V_{xx} , such as the skewness, can lead to deviations from the universal pattern. The normalized skewness (and higher moments) of V_{xx} approach zero in accordance with the central limit theorem in the regime of strongly overlapping potential bumps, but the skewness can be substantial for low bump density (i.e., where the typical bump separation is large compared to the bump width).

High-accuracy numerical simulations are challenging for 2D scattering in this dilute regime due to large statistical

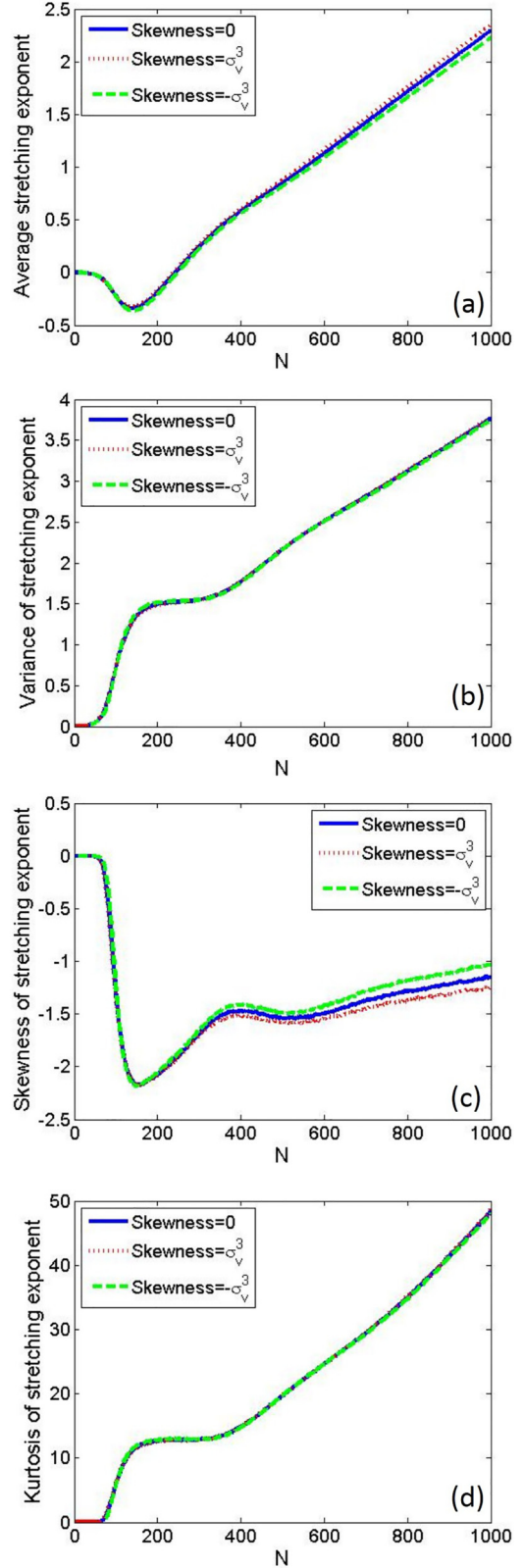


FIG. 6. Moments of the stretching exponent α in a 1D kicked model where the average of the v is zero, the variance is $\sigma_v = 0.002$, and the skewness is $-\sigma_v^3$, 0 , or σ_v^3 . Panels (a), (b), (c), and (d) show the mean, variance, skewness, and kurtosis of the stretching exponent, respectively. Accurate statistics are obtained by averaging over 100 million realizations of the ensemble in each case.

noise. However, any distribution of V_{xx} , including a strongly non-Gaussian distribution, can be easily simulated in the 1D kicked model, and using the correspondence between the kicked 1D model and small-angle 2D scattering we can predict the effect of higher moments of the V_{xx} distribution in 2D scattering.

As we observe in Fig. 6, the skewness of the V_{xx} distribution does not significantly change the length scale where the strongest focusing occurs, but does slightly modify the large-time behavior, i.e., the value of the maximum Lyapunov exponent. The even moments of the stretching exponent distribution seem to be robust to skewness effects.

IV. CONCLUSION

We have seen that the connection between ray densities and stretching exponents, previously discussed in Ref. [27], can be extended to a wide variety of physical contexts. Specifically, we have seen semianalytically and confirmed numerically that the evolution of the stretching exponent distribution with propagation distance is identical for a broad range of dispersion relations governing the ray propagation, as long as the disorder is weak and the angular ray spread is narrow. We have obtained analytically, in Eq. (17), the scaling factor for the propagation distance needed to relate stretching exponent evolutions for different dispersion relations.

Furthermore, we have shown that, under the same assumptions of weak disorder and narrow angular spread, the stretching exponent distributions are independent of the form of the spatial correlation function describing the random potential. Again, we have obtained an analytical form in Eq. (40) for mapping the stretching exponent evolution obtained for a given disorder ensemble into one appropriate for a different

disorder correlation. The same scaling describes correctly the short-time behavior of the stretching exponent, the maximal Lyapunov exponent (MLE) displayed in Table I, which governs large-time behavior, and the intermediate-time evolution.

The universal scaling factor combines contributions from the strength of the second derivatives of the potential and from their correlation along the forward direction. We note that wider angular ray spread or stronger potential or nonlinear effects will induce higher order terms in the evolution of stretching exponents, and will therefore lead to deviations of the stretching exponent evolution from the universal pattern.

Mathematically, the stretching exponents in 2D ray scattering in random disorder can be obtained by multiplying a sequence of random Jacobian matrices. For small scattering angle, the equations governing the time evolution are shown to be equivalent to those for 1D scattering in a time-dependent potential. Furthermore, up to a numerical prefactor, the 1D model in a correlated potential is seen to be equivalent to a sequence of uncorrelated kicks, which does not require a potential to be constructed at all and is very efficient for numerical simulations. The 1D kicked model proves to be very convenient for studying how the evolution of the stretching exponent distribution may be affected both by correlations and by the distribution of kick strengths.

ACKNOWLEDGMENTS

This research was supported in part using high performance computing (HPC) resources and services provided by Technology Services at Tulane University, New Orleans. This work was supported in part by the National Science Foundation under Grant No. PHY-1205788.

-
- [1] M. S. Longuet-Higgins, The statistical analysis of a random, moving surface, *Philos. Trans. R. Soc. Ser. A* **249**, 321 (1957).
 - [2] K. Trulsen and K. B. Dysthe, A modified nonlinear Schrödinger equation for broader bandwidth gravity waves on deep water, *Wave Motion* **24**, 281 (1996).
 - [3] K. B. Dysthe, Note on a modification to the nonlinear Schrödinger equation for application to deep water waves, *Proc. R. Soc., Ser. A* **369**, 105 (1979).
 - [4] B. S. White and B. Fornberg, On the chance of freak waves at sea, *J. Fluid Mech.* **355**, 113 (1998).
 - [5] H. Dankert, J. Hortsman, S. Lehner, and W. Rosenthal, Detection of wave groups in SAR images and radar image sequences, *IEEE Trans., Geosci. Remote Sens.* **41**, 1437 (2003).
 - [6] E. J. Heller, L. Kaplan, and A. Dahlen, Refraction of a Gaussian seaway, *J. Geophys. Res.* **113**, C09023 (2008).
 - [7] R. Höhmann, U. Kuhl, H. J. Stöckmann, L. Kaplan, and E. J. Heller, Freak waves in the linear regime: A microwave study, *Phys. Rev. Lett.* **104**, 093901 (2010).
 - [8] M. A. Topinka, B. J. LeRoy, R. M. Westervelt, S. E. J. Shaw, R. Fleischmann, E. J. Heller, K. D. Maranowski, and A. C. Gossard, Coherent branched flow in a two-dimensional electron gas, *Nature (London)* **410**, 183 (2001).
 - [9] M. P. Jura, M. A. Topinka, L. Urban, A. Yazdani, H. Shtrikman, L. N. Pfeiffer, K. W. West, and D. Goldhaber-Gordon, Unexpected features of branched flow through high-mobility two-dimensional electron gases, *Nat. Phys.* **3**, 841 (2007).
 - [10] K. E. Aidala, R. E. Parrott, T. Kramer, E. J. Heller, R. M. Westervelt, M. P. Hanson, and A. C. Gossard, Imaging magnetic focusing of coherent electron waves, *Nat. Phys.* **3**, 464 (2007).
 - [11] D. Maryenko, F. Ospald, K. von Klitzing, J. H. Smet, J. J. Metzger, R. Fleischmann, T. Geisel, and V. Umansky, How branching can change the conductance of ballistic semiconductor devices, *Phys. Rev. B* **85**, 195329 (2012).
 - [12] L. Kaplan, Statistics of branched flow in a weak correlated random potential, *Phys. Rev. Lett.* **89**, 184103 (2002).
 - [13] M. V. Berry, Tsunami asymptotics, *New J. Phys.* **7**, 129 (2005).
 - [14] M. V. Berry, Focused tsunami waves, *Proc. R. Soc. A* **463**, 3055 (2007).
 - [15] S. Yu. Dobrokhotov, S. Y. Sekerzh-Zenkovich, B. Tirozzi, and T. Ya. Tudorovskii, Description of tsunami propagation based on the Maslov canonical operator, *Dokl. Math.* **74**, 592 (2006).
 - [16] A. Patsyk, U. Sivan, M. Segev, and M. A. Bandres, Observation of branched flow of light, *Nature (London)* **583**, 60 (2020).
 - [17] F. T. Arecchi, U. Bortolozzo, A. Montina, and S. Residori, Granularity and inhomogeneity are the joint generators of optical rogue waves, *Phys. Rev. Lett.* **106**, 153901 (2011).

- [18] C. Bonatto, M. Feyereisen, S. Barland, M. Giudici, C. Masoller, J. R. Rios Leite, and J. R. Tredicce, Deterministic optical rogue waves, *Phys. Rev. Lett.* **107**, 053901 (2011).
- [19] M. A. Wolfson and S. Tomsovic, On the stability of long-range sound propagation through a structured ocean, *J. Acoust. Soc. Am.* **109**, 2693 (2001).
- [20] J. A. Colosi, A. B. Baggeroer, T. G. Birdsall, C. Clark, B. D. Cornuelle, D. Costa, B. D. Dushaw, M. A. Dzieciuch, A. M. G. Forbes, B. M. Howe *et al.*, A review of recent results on ocean acoustic wave propagation in random media: Basin scales, *IEEE J. Oceanic Eng.* **24**, 138 (1999).
- [21] S. Barkhofen, J. J. Metzger, R. Fleischmann, U. Kuhl, and H.-J. Stöckmann, Experimental observation of a fundamental length scale of waves in random media, *Phys. Rev. Lett.* **111**, 183902 (2013).
- [22] J. J. Metzger, R. Fleischmann, and T. Geisel, Universal statistics of branched flows, *Phys. Rev. Lett.* **105**, 020601 (2010).
- [23] J. J. Metzger, R. Fleischmann, and T. Geisel, Statistics of extreme waves in random media, *Phys. Rev. Lett.* **112**, 203903 (2014).
- [24] H. Degueldre, J. J. Metzger, E. Schultheis, and R. Fleischmann, Channeling of branched flow in weakly scattering anisotropic media, *Phys. Rev. Lett.* **118**, 024301 (2017).
- [25] J. Štavina and P. Bokes, Quantum and classical branching flow in space and time, *Phys. Rev. A* **106**, 052215 (2022).
- [26] E. J. Heller, R. Fleischmann, and T. Kramer, Branched flow, *Phys. Today* **74**, 44 (2021).
- [27] S. Chen and L. Kaplan, Ray-stretching statistics and hot-spot formation in weak random disorder, *Entropy* **25**, 161 (2023).
- [28] J. Meibohm, K. Gustavsson, J. Bec, and B. Mehlig, Fractal catastrophes, *New J. Phys.* **22**, 013033 (2020).
- [29] H. Schomerus, and M. Titov, Statistics of finite-time Lyapunov exponents in a random time-dependent potential, *Phys. Rev. E* **66**, 066207 (2002).
- [30] R. Livi, A. Politi, and S. Ruffo, Scaling-Law for the maximal Lyapunov exponent, *J. Phys. A: Math. Gen.* **25**, 4813 (1992).
- [31] M. Brack and R. Bhaduri, *Semiclassical Physics* (CRC Press, Boca Raton, FL, 2003).
- [32] M. S. Longuet-Higgins, The generation of capillary waves by steep gravity waves, *J. Fluid Mech.* **16**, 138 (1963).
- [33] V. A. Kulkarny and B. S. White, Focusing of waves in turbulent inhomogeneous media, *Phys. Fluids* **25**, 1770 (1982).